Optimal corneal ablation for eyes with arbitrary Hartmann–Shack aberrations

Stanley A. Klein

School of Optometry, University of California, Berkeley, Berkeley, California 94720

Received January 15, 1998; revised manuscript received March 30, 1998; accepted April 2, 1998

New technologies for accurately measuring corneal shape and full eye aberrations are now available. An algorithm that uses these technologies to predict the amount of ablation needed to produce a corneal surface that optimally focuses light is developed. It is found that knowledge of the aberrations is far more important than knowledge of corneal shape. Neglect of corneal shape information introduces an error of less than approximately 0.05 μm in the optimal ablation depth. Neglect of the aberrations is a different story. Small changes in the aberration structure, such as going from the optimal ablation to a spherical ablation, introduce ablation changes of greater than 10 μm. It is argued that there are many occasions when less ablation can lead to improved image quality. © 1998 Optical Society of America [S0740-3232(98)00309-3]

OCIS codes: 080.1010, 110.2990, 120.3890, 170.1020, 170.4460, 330.4460.

1. INTRODUCTION

The precision with which refractive surgery can modify corneal shape is constantly improving.[1] In addition, technologies are now available for accurately measuring corneal shape[1,2] and the full optical aberrations of the eye.[3,4] With this increased precision of surgery and measurement, the natural question becomes, Which corneal shape optimizes vision? The original purpose of this paper was to discuss how the two technologies (corneal topography and aberration measurement devices) can be combined to specify a new corneal shape with ideal optics. To my surprise, my research showed that the aberrations alone are sufficient to accurately specify the optimal corneal ablation. The shape of the corneal surface is irrelevant. The present paper has three objectives: First, to present an algorithm for calculating the optimal amount of ablation such that all rays from a distant object focus at the same retinal point; second, to demonstrate that corneal shape information is not needed for determining the optimal corneal ablation pattern; third, to demonstrate that a small amount of residual spherical aberration after ablation may be desirable for reducing the depth of ablation, with a side benefit of extending the depth of focus.

2. THEORY AND METHODS

Our approach starts with the Hartmann–Shack (HS) data, so it is useful to describe the HS method.[3–5] The HS goal is to describe the shape of the wave front that is emerging from the eye, and which originates from a tiny point of illumination on the retina. The HS sensor consists of between 50 and 200 tiny lenslets that focus the rays emerging from small segments of the cornea onto a CCD array, as shown in Fig. 1(a). The lateral location of the focus from each lenslet specifies the local slope of the emerging wave. From the slope, the wave-front phase can be calculated. Knowledge of the wave-front phase plus the slope allows us to calculate the amount of corneal ablation needed for an optimal corneal shape. The importance of the high-quality HS information cannot be overemphasized. The recent demonstrations by Liang and Williams of the accuracy[4] and by Liang *et al.* of the capabilities[5] of this method for measuring aberrations are most impressive.

A. Exact Algorithm

The steps of our algorithm are as follows.

Step 1. The starting data are of two sorts. First are the HS data, which specify the location $(x_{\mathrm{HS}}, y_{\mathrm{HS}}, z_{\mathrm{HS}})$ of a given HS lenslet and the direction $(\hat{\mathbf{V}}_{\mathrm{HS}})$ at each lenslet of the ray emerging from the cornea (we use the convention that three-dimensional vectors are shown in boldface letters). Our coordinate system has the corneal vertex as the origin, with the corneal normal at the vertex pointing rightward, in the $+z$ direction. That is, the corneal normal is pointing into the eye, not away from the eye, since the eye is facing to the left. The second sort of input data is knowledge of the corneal shape and corneal index of refraction. An outcome of our analysis will be that knowledge of corneal shape has a negligible effect on the amount of ablation needed for optimal vision.

Step 2. Do a backwards ray tracing, starting with the known slope of each ray based on the HS data. Although the actual rays in the HS experiment start at the retina, go through the eye, and then hit the HS sensors, in this paper the rays are described as going in the opposite direction. They will start at the HS plane, traveling in the direction of $\hat{\mathbf{V}}_{\mathrm{HS}}$. The first challenge is to calculate the intersection of the ray with the cornea. This can be done in an iterative calculation.

Step 2.1. Start with an initial guess for the corneal position z_c as a function of x_c and y_c. A reasonable starting point is to use $x_c = x_{\mathrm{HS}}$ and $y_c = y_{\mathrm{HS}}$. We then know z_c, since we are assuming that we know the corneal shape as a function of x_c and y_c based on the topography information.

0740-3232/98/092580-09$15.00

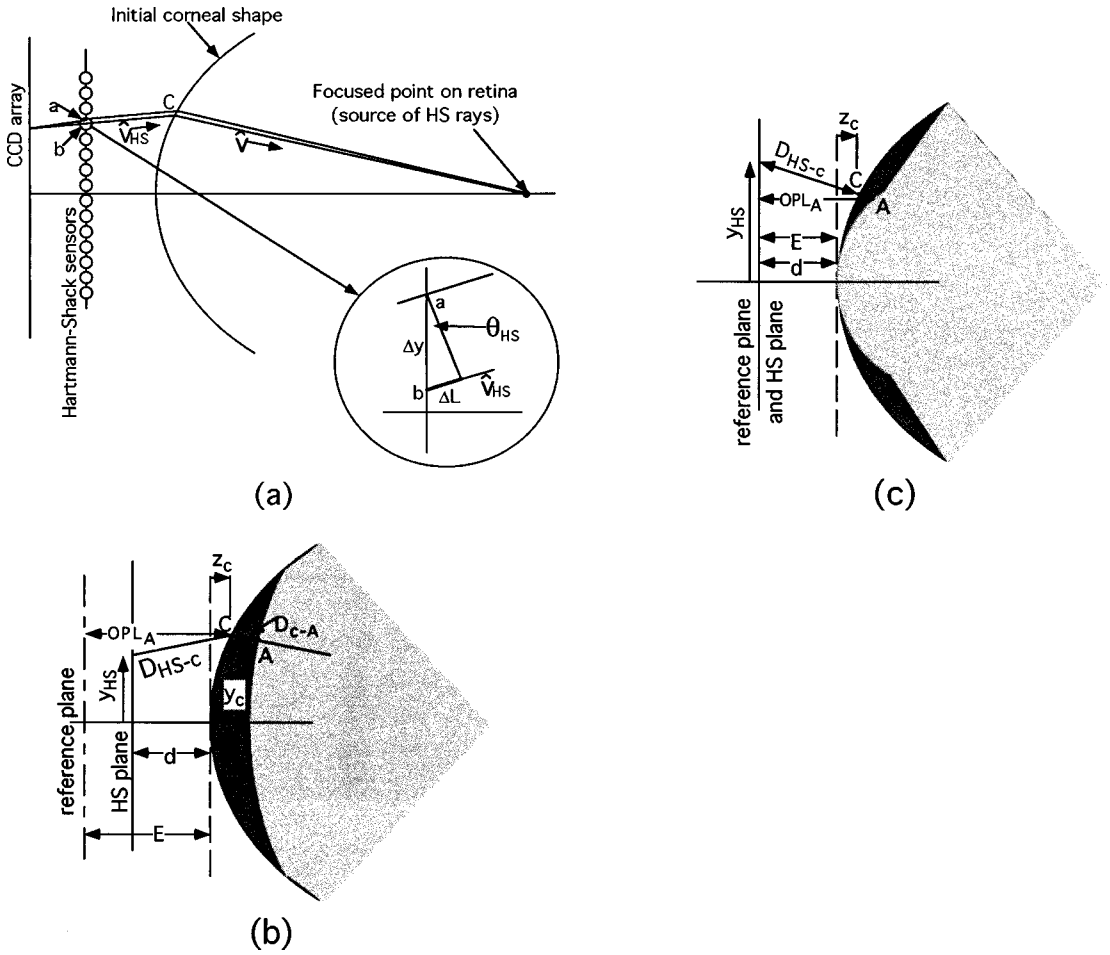

Fig. 1. Geometry of the HS sensors in relation to measuring aberrations of the eye. Light is focused on the retina from a light source that is not shown. The light not absorbed by the retina then travels to the left, being refracted by the lens and cornea of the eye. After emerging from the eye, it gets focused by one of the HS lenslets onto the CCD array. For simplicity of discussion, the rays are considered to travel in reverse. Thus Eqs. (1) and (2) of the present algorithm are based on rays traveling from the HS sensor toward the cornea in the direction $\hat{\mathbf{V}}_{\mathrm{HS}}$. After the rays are refracted by the cornea, their direction becomes $\hat{\mathbf{V}}$, as indicated in (a). Inset: Blown-up version of one of the lenslets, with two adjacent rays shown striking the HS plane at points a and b. The triangle in the inset is used in the derivation of Eq. (9). (b) shows a portion of (a). Dark-shaded region, the region of the cornea that is to be ablated for a myopic correction. Light-shaded region, the eye after the ablation. The distance from the HS sensor to the cornea, $D_{\mathrm{HS}-c}$, is calculated by an iterative method in step 2 of the algorithm. The distance from the preablated to the postablated cornea, D_{c-A}, is calculated in step 7. In actual practice the HS array is placed conjugate to the eye's entrance pupil (roughly 3 mm behind the cornea), by use of relay lenses, rather than in front of the cornea as shown in this diagram. (c) Similar to (b), except that it is for correcting a hyperopic eye. In (c) the reference plane for measuring the distance to the postablated eye is coincident with the HS plane. In (b) the reference plane is to the left of the HS plane, resulting in a deeper ablation near the axis than is the case with hyperopic correction.

Step 2.2. Calculate the x and y corneal positions on the basis of the known x and y components of the slope of each ray, $S_{\mathrm{HS}-x}$, $S_{\mathrm{HS}-y}$ as given by the HS sensors:

$$x_c = x_{\mathrm{HS}} + (z_c - z_{\mathrm{HS}})S_{\mathrm{HS}-x}, \tag{1a}$$

$$y_c = y_{\mathrm{HS}} + (z_c - z_{\mathrm{HS}})S_{\mathrm{HS}-y}, \tag{1b}$$

where the components of the slope S_{HS} are related to the components of the unit vector, $\hat{\mathbf{V}}_{\mathrm{HS}} = (V_{\mathrm{HS}-x}, V_{\mathrm{HS}-y}, V_{\mathrm{HS}-z})$, by

$$S_{\mathrm{HS}-x} = V_{\mathrm{HS}-x}/V_{\mathrm{HS}-z}, \tag{2a}$$

$$S_{\mathrm{HS}-y} = V_{\mathrm{HS}-y}/V_{\mathrm{HS}-z}. \tag{2b}$$

Step 2.3. Recalculate the corneal position z_c on the basis of the new x_c and y_c positions. If this position, z_c, is different (to within a tolerance) from its previous value, then go back to step 2.2.

Since the rays in question are nearly parallel to the axis, the iterative algorithm was found to converge to an accuracy of 10^{-6} mm in approximately four iterations. The resulting corneal point will be called (x_c, y_c, z_c).

Step 3. Use Snell's law to calculate the direction of each ray inside the cornea. For this three-dimensional problem, Snell's law is given by

$$n_2\hat{\mathbf{V}} = n_1\hat{\mathbf{V}}_{\mathrm{HS}} + \gamma_{\mathrm{HS}}(x_c, y_c)\hat{\mathbf{n}}(x_c, y_c), \tag{3}$$

where $\hat{\mathbf{V}}_{\mathrm{HS}}$ is the unit vector specifying the ray direction in front of the eye, $\hat{\mathbf{V}}$ is the unit vector specifying the ray direction of the ray in the cornea, and $\hat{\mathbf{n}}$ is the unit vector of the corneal normal (pointing mainly in the $+z$ direction). One validates the presence of the indices of refraction, n_1 and n_2, that appear in Eq. (3) by taking the cross product of $\hat{\mathbf{n}}$ with both sides of Eq. (3), which gives Snell's law:

$$n_2 \sin(\theta_2) = n_1 \sin(\theta_1). \tag{4}$$

For the air–cornea interface, the indices of refraction are $n_1 = 1$ and $n_2 = 1.376$. It is important to use $n_2 = 1.376$ in this context because it is the cornea that is to be ablated, so we must use its index. The angles θ_1 and θ_2 are the incident and refracted angles that the ray makes with the corneal normal.

The dot product of $\hat{\mathbf{n}}$ with both sides of Eq. (3) is used to determine the value of γ_{HS} needed in Eq. (3):

$$\gamma_{\mathrm{HS}} = n_2 \cos(\theta_2) - n_1 \cos(\theta_1), \tag{5}$$

where $\cos(\theta_2)$ and $\cos(\theta_1)$ are given by the dot products of $\hat{\mathbf{n}}$ with $\hat{\mathbf{V}}$ and $\hat{\mathbf{V}}_{\mathrm{HS}}$. A more symmetric way of writing Eqs. (3) and (5) is $n_2\hat{\mathbf{n}}x(\hat{\mathbf{n}}x\hat{\mathbf{V}}) = n_1\hat{\mathbf{n}}x(\hat{\mathbf{n}}x\hat{\mathbf{V}}_{\mathrm{HS}})$, based on the identity $\mathbf{A}x(\mathbf{B}x\mathbf{C}) = \mathbf{B}(\mathbf{A}*\mathbf{C}) - \mathbf{C}(\mathbf{A}*\mathbf{B})$, where $*$ is the dot product.

This completes the information needed for ray tracing, since $\cos(\theta_1)$ is known because $\hat{\mathbf{n}}$ and $\hat{\mathbf{V}}_{\mathrm{HS}}$ are given, and θ_2 can be expressed in terms of θ_1 from Snell's law [Eq. (4)]. Thus, with knowledge of $\hat{\mathbf{n}}(x_c, y_c)$, obtained from corneal topography, and $\hat{\mathbf{V}}_{\mathrm{HS}}$, obtained from the HS information, we can calculate $\hat{\mathbf{V}}$, the desired ray within the cornea.

Step 4. To calculate the optimal corneal shape, we need to know the shape of the wave front. This has been done in two different ways. The first method uses Snell's law to ray trace each ray from the HS sensors back into the cornea. Then, knowing the ray slope, $\hat{\mathbf{V}}$, we first calculate the wave front inside the cornea and then calculate the ablation amount needed to generate that wave front. This method has the advantage that it is conceptually simple. The disadvantage is that the step for calculating the wave front requires a number of iterations, since the x, y position of a given ray at the wave front is not known. We start the second method by generating the wave-front phase at the HS sensors and then calculating the amount of ablation that produces this wave front for incoming plane waves. The two methods produce ablations that differ by less than 10^{-3} μm. Both methods produce perfect refraction in that all incoming rays have the same focal point to within 10^{-10} μm. The details of the second method are presented here because it is more instructive and because it avoids the step that requires iterations.

The ray slopes at the HS sensors can be converted to the phase at the sensors by a method that is similar to that of Southwell[6] and Liang.[7] In steps 5–7 we will be calculating the path length from different points on the HS sensors to the cornea. We need to express the phase at the HS sensors in units of path length. This can be done by multiplication of the phase in radians by $\lambda/2\pi$ to convert the phase into distance units:

$$L(x_{\mathrm{HS}}, y_{\mathrm{HS}}) = \lambda/(n_1 2\pi)\phi(x_{\mathrm{HS}}, y_{\mathrm{HS}}), \tag{6}$$

where λ/n_1 is the wavelength of light in air ($n_1 = 1$ in our case). Since we are not dealing with interference or diffraction, only the path length L will enter our equations, and there is no explicit wavelength dependence.

The path-length phase in Eq. (6) can be written as a two-dimensional polynomial with linear coefficients:

$$L(x_{\mathrm{HS}}, y_{\mathrm{HS}}) = \sum_{j,k} a_{jk} x_{\mathrm{HS}}^j y_{\mathrm{HS}}^k. \tag{7}$$

The subtle, surprisingly simple part of the calculation is the question of how to relate $L(x_{\mathrm{HS}}, y_{\mathrm{HS}})$ to the HS information that consists of the slope of the rays at the HS plane. The inset in Fig. 1 is a blowup of the region in which the two closely spaced, parallel rays hit the HS array. We need to know the path-length phase difference, ΔL, between the two points a and b. The phase difference ΔL can be analyzed in terms of its components along the direction of the ray and perpendicular to the direction of the ray. Only the component along the direction of the ray will contribute to the path length. Thus, for a small interval, ΔL can be written as

$$\Delta L = \hat{\mathbf{V}}_{\mathrm{HS}} * \Delta \mathbf{r}_{\mathrm{HS}} \tag{8}$$

$$= V_{\mathrm{HS}-x}\Delta x_{\mathrm{HS}} + V_{\mathrm{HS}-y}\Delta y_{\mathrm{HS}}, \tag{9}$$

where $\hat{\mathbf{V}}_{\mathrm{HS}}$ is the unit vector in the direction of the ray and $\Delta\mathbf{r}_{\mathrm{HS}}$ is a differential vector in the HS plane. The components $V_{\mathrm{HS}-x}$ and $V_{\mathrm{HS}-y}$ are the direction cosines between $\hat{\mathbf{V}}_{\mathrm{HS}}$ and the x and y axes. They are the same quantities that were used in Eqs. (1). For a ray in the y–z plane, as shown in Fig. 1, only the $V_{\mathrm{HS}-y}\Delta y_{\mathrm{HS}}$ term would be present, and $V_{\mathrm{HS}-y} = \sin(\theta_{\mathrm{HS}})$, where $\mathrm{d}z/\mathrm{d}y = \tan(\theta_{\mathrm{HS}})$, is the slope measured by the HS sensor.

The wave-front slope can now be used to calculate the wave-front expansion coefficients a_{jk}. The slope can be expanded as

$$V_x(x_{\mathrm{HS}}, y_{\mathrm{HS}}) = \partial L/\partial x_{\mathrm{HS}} = \sum_{j,k} j a_{jk} x_{\mathrm{HS}}^{j-1} y_{\mathrm{HS}}^k, \tag{10a}$$

$$V_y(x_{\mathrm{HS}}, y_{\mathrm{HS}}) = \partial L/\partial y_{\mathrm{HS}} = \sum_{j,k} k a_{jk} x_{\mathrm{HS}}^{j} y_{\mathrm{HS}}^{k-1}. \tag{10b}$$

The coefficients a_{jk} in Eqs. (10) are calculated by linear regression based on knowledge of the direction cosines, V_x and V_y, at the points x_{HS} and y_{HS} for each ray specified by the HS sensors. If there are N_{HS} x and y locations of the HS sensors, then there are $2N_{\mathrm{HS}}$ equations to determine the N_{coef} unknowns, where N_{coef} are the number of coefficients, a_{jk}, in the expansion. The coefficients a_{jk} can then be directly obtained by linear regression through the standard matrix inversion method.

Step 5. We are now ready to propagate the phase wave front, L, from the HS array to the cornea and then onward to the surface A, which is destined to become the new ablated cornea. The optical path length (OPL), including the initial phase L, is given by

$$\mathrm{OPL}_{\mathrm{HS}} = L(x_{\mathrm{HS}}, y_{\mathrm{HS}}) + D_{\mathrm{HS}-c} + nD_{c-A}, \tag{11}$$

where $L(x_{\mathrm{HS}}, y_{\mathrm{HS}})$ is given by Eq. (7) and n_1 and n_2 are taken to be 1 and n, respectively. $D_{\mathrm{HS}-c}$, the distance that the ray travels from the HS plane to the point at which it intersects the cornea, is given by

$$D_{\mathrm{HS}-c} = (z_c + d)/\cos(\theta_{\mathrm{HS}}). \tag{12}$$

The location of the corneal point (x_c, y_c, z_c) was calculated in step 2 above, d is the distance from the HS plane to the vertex plane, and z_c is the distance from the vertex

plane to the cornea (calculated in step 2). The angle θ_{HS} is the angle that the incoming ray makes with the axis; it is the angle measured by the HS sensors:

$$\cos(\theta_{\mathrm{HS}}) = V_{\mathrm{HS}-z}, \tag{13}$$

where $V_{\mathrm{HS}-z}$ is the z component of the unit vector specifying the direction of the incoming ray. The distance D_{c-A} in Eq. (11) is the distance that the ray travels from the preablation corneal point to the point at which it hits the corneal surface after ablation. The various distances are shown in the diagrams in Figs. 1(b) and 1(c) for the cases of myopic and hyperopic ablations, respectively. So far, the distance D_{c-A} is unknown. It is the quantity that we are trying to calculate, since once it is known we would know the location of the final surface, which allows us to calculate the amount of ablation needed. The factor n is present in Eq. (11) because we are calculating the optical phase or the time traveled by the ray rather than simply its total distance traveled.

Step 6. Equation (11) shows how to calculate the optical phase of each ray at the intended ablated corneal surface, based on information provided by the HS sensors for the preablated cornea. Now we must do a similar calculation for the postablated cornea. Our goal is to determine the unique ablated shape that equates both phase maps. For the postablated cornea we wish to have an incoming plane wave that is traveling in the z direction come to the same focus on the retina as the rays shown in Fig. 1. The optical path length for the ablated cornea, OPL_A, from a reference plane located a distance E in front of the vertex plane [see Figs. 1(a) and 1(b)], is given by

$$\mathrm{OPL}_A = E + z_c + D_{c-A}\cos(\theta_c), \tag{14}$$

where θ_c is the angle that the ray makes with the axis after refraction by the cornea. This angle is given by

$$\cos(\theta_c) = V_z, \tag{15}$$

where V_z has been calculated by Snell's law in Eq. (3). As is discussed below, the aberration structure might make it advantageous to slightly tilt the reference plane so that E becomes a linear function of x_{HS} and y_{HS}.

Step 7. We can now solve for D_{c-A} by equating Eqs. (11) and (14), both of which specify the optical phase at the ablated cornea:

$$L + (z_c + d)/V_{\mathrm{HS}-z} + nD_{c-A} = E + z_c + D_{c-A}V_z, \tag{16}$$

where we have used Eq. (12) for $D_{\mathrm{HS}-c}$. This equation can be solved to obtain D_{c-A}:

$$D_{c-A} = [E + z_c - L - (z_c + d)/V_{\mathrm{HS}-z}]/(n - V_z). \tag{17}$$

Each of the quantities in Eq. (17), except for E and n, depends on the chosen ray, specified by x_{HS} and y_{HS}.

The location of the reference plane, E, controls the depth of ablation. For a hyperopic eye [Fig. 1(c)], E is chosen so that the ablation depth D_{c-A} never goes negative but has a minimum value of zero (a point of no ablation) near the center of the ablation. This condition gives

$$E = -\min[z_c - L - (z_c + d)/V_{\mathrm{HS}-z}], \tag{18}$$

where the minimum is taken over all the rays within the ablation zone. For an eye in which the pupil is centered on the VK axis, the line of sight will be normal to the cornea at the vertex ($V_{\mathrm{HS}-z} = 1$ at the vertex). Furthermore, for a hyperopic eye, L will be minimum at the vertex, so Eq. (18) implies that $E = d$ for a hyperopic, symmetric eye. That is, the reference plane is the plane with the HS sensors. For myopic eyes or hyperopic eyes that are not symmetric, there is a slight displacement of the reference plane from the HS plane.

If Eq. (18) is used for a myopic eye [see Fig. 1(b)], then a point of zero ablation will occur at the periphery of the ablation zone. For the present discussion we take the ablation zone to have a radius of 3 mm. In the presence of refractive astigmatism, all but one (or two) of the points at the 3-mm radius would have ablation. For myopic eyes an alternative method for specifying E is to choose E so that, at the 3-mm radius, the ablation is just beginning. The condition can be written as

$$E = -\max[z_c - L - (z_c + d)/V_{\mathrm{HS}-z}], \tag{19}$$

where the maximum is taken only over all the rays at the 3-mm boundary. This method produces a smoother transition to the unablated eye, but it has a smaller ablation zone. In the case in which Eq. (18) is used some ablation outside the 3-mm radius would be needed if a smooth transition were desired, because there could be substantial ablation at the 3-mm radius along most meridia.

Step 8. The final step is to use the quantity D_{c-A} to calculate the coordinates of the new ablated corneal surface (x_A, y_A, z_A):

$$x_A = x_c + D_{c-A}V_x, \tag{20a}$$

$$y_A = y_c + D_{c-A}V_y, \tag{20b}$$

$$z_A = z_c + D_{c-A}V_z. \tag{20c}$$

To calculate the amount of ablation at corneal points x_A, y_A we must first calculate the corneal height at that point, $z_c(x_A, y_A)$. It turns out that the correction that is due to the angle of the vector $\hat{\mathbf{V}}$ is negligible, so that D_{c-A} is an accurate estimate of the needed ablation.

The above algorithm was checked in the following manner. A single-surface schematic eye with a spherical front surface was assumed. The retina was displaced from the paraxial focus (to give the eye some refractive error). A variety of corneal curvatures and retinal locations were chosen. A large group of rays was ray traced, starting at the axial point on the retina and ending at the HS sensor. Snell's law was used at the cornea. Once the HS information was generated by this procedure, steps 1–8 of the above algorithm were then used to calculate the ablation. Finally, rays from a distant object were ray traced through the ablated cornea to determine where they hit the axis. They all had the identical focal length to within one part in 10^{14}. So the algorithm works.

B. Simpler Approximate Algorithm

In Subsection 3.A we compare the exact ablation amount given by the above algorithm with an ablation amount given by a much simpler algorithm that ignores the cor-

neal shape. The goal is to modify Eq. (17) by removing the quantities z_c and V_z that depend on corneal shape. The quantity $n - V_z$ can be set to $n - 1$, since $V_z - 1$ is small compared with $n - 1$. By setting z_c to zero we are omitting the quantity $z_c(1 - 1/V_{\mathrm{HS}-z})$ from Eq. (17). A calculation similar to what will be done in relation (23) indicates that this quantity is negligible. The validity of this approximation is justified in Section 3. In this paraxial approximation, D_{c-A}, the distance from the cornea (the $z = 0$ plane) to the ablation point A becomes, from Eq. (17),

$$D(x, y) = [E - d/V_{\mathrm{HS}-z} - L(x, y)]/(n - 1). \quad (21)$$

The coordinates x, y do not need subscripts because in this approximation all rays are sufficiently close to being parallel to the axis. The quantity E is determined as before [see Eqs. (18) or (19)]. Use of the condition in Eq. (18) allows Eq. (21) to be written as

$$D(x, y) = \{d[\max(1/V_{\mathrm{HS}-z}) - 1/V_{\mathrm{HS}-z}] + \max(L) - L(x, y)\}/(n - 1), \quad (22)$$

where the maximum is taken over all the rays. The quantity that depends on $V_{\mathrm{HS}-z} = \cos(\theta)$ is so close to unity that one is tempted to neglect that term in Eq. (22). However, the quantity is not negligible because the dominant terms cancel, as can be seen from the following calculation:

$$d[\max(1/V_{\mathrm{HS}-z}) - 1/V_{\mathrm{HS}-z}]/(n - 1) \approx d[1 - \cos(\theta)]/(n - 1) \approx d\,\theta^2/2(n - 1) \approx -3(0.003 \times 5)^2/2(n - 1) \approx -1.0\ \mu\mathrm{m}. \quad (23)$$

For this calculation we have assumed a 5-diopter incoming vergence, which gives an angle of $\theta = 0.003 \times 5 = 0.015$ rad at a radius of 3 mm from the axis. The distance from the HS sensors to the corneal vertex is taken to be $d = -3$ mm, based on the Liang–Williams[4] design of using relay lenses to place the HS sensors at the entrance pupil of the eye. For simplicity of presentation, Figs. 1(a)–1(c) each shows the HS plane in front of the cornea. The same derivation that was done above is valid for the placement of the sensors behind the cornea, at the entrance pupil. The only modification is that the sign of d is reversed. The quantity in relation (23) is much larger than the error made by the other approximations. Thus Eq. (22) must keep the $d/V_{\mathrm{HS}-z}$ terms.

The quantity shown in Eq. (22) is the amount of ablation that is predicted by our simplified model. In Subsection 3.A we compare the ablations calculated by the exact and the approximate methods. This comparison shows that the approximation of neglecting the precise corneal shape is quite good.

3. RESULTS

A. Comparison between Exact and Approximate Formulas for Ablation

Figure 2 is a comparison of the amount of ablation obtained from the exact algorithm in Eqs. (1)–(20) with the simplified approximate algorithm in relations (21)–(23). For this figure, HS data are taken with HS sensor locations within a disk of diameter 6 mm centered on the axis. A maximum radius of $r = 3$ mm is chosen to maintain close correspondence with photorefractive keratectomy (PRK). In our example the slopes of the rays detected by the HS sensors are taken as coming from a 5.00-D myope, so that the object point conjugate to the retina is $u = -200$ mm in front of the cornea. The formula for the maximum ablation depth for this cornea is

$$\text{depth} = Pr^2/2(n - 1) = 5 \times 3^2/(2 \times 0.376) \approx 60\ \mu\mathrm{m}, \quad (24)$$

where $n = 1.376$, the corneal index, because we are ablating the cornea.

The ray slope measured by the HS sensors, which is the main input to the algorithm described in Section 2, was taken to be

$$S_{\mathrm{HS}-x} = x_{\mathrm{HS}}/(z_{\mathrm{HS}} - u), \quad (25a)$$

$$S_{\mathrm{HS}-y} = y_{\mathrm{HS}}/(z_{\mathrm{HS}} - u), \quad (25b)$$

where $(x_{\mathrm{HS}}, y_{\mathrm{HS}}, z_{\mathrm{HS}})$ is the location on the HS sensor. The location of the HS plane is taken to be in the entrance pupil plane[4] with $z_{\mathrm{HS}} = d = -3$ mm, as is discussed below relation (23). The negative sign is there because our equations were originally developed for a positive d that was anterior to the cornea. For these HS data the ablation pattern was calculated with a variety of rotationally symmetric ellipsoidal corneal shapes. The abscissa is R, the apical radius of curvature, which ranges from 6.5 to 10.0 mm. The p value of the ellipse was either 0 (a parabola) or 1 (a sphere), as indicated on the two curves in Fig. 2. The p value is related to eccentricity, e, by

$$p = 1 - e^2. \quad (26)$$

Several steps of the exact algorithm [step 2.3 and the negligible correction given below Eq. (20)] require a calculation of the corneal height in terms of x and y. For an axi-

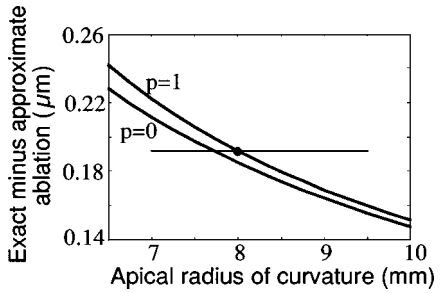

Fig. 2. Maximum difference in ablation owing to the exact algorithm versus the algorithm that ignores corneal shape by replacing the cornea with a flat plane. The corneal shapes tested were axially symmetric ellipsoids whose apical radii ranged from $R = 6.5$ to $R = 10$ mm, shown on abscissa, and whose p value (oblateness) was either 0 (paraboloid) or 1 (sphere). The plots show that a maximum error of 0.25 μm would be made by this approximation. The horizontal line that intersects the $p = 1$ curve at $R = 8$ mm provides an estimate of the error incurred by replacement of the flat plane approximation with an approximate shape (an 8-mm sphere in this case). When a reasonable corneal shape is used together with the exact algorithm, the ablation error is reduced to less than 0.05 μm, which is smaller than the intrinsic errors associated with estimating the aberrations.

ally symmetric ellipsoid such as that used in the calculations for Fig. 2, the height is

$$z = r^2/[R + (R^2 - pr^2)^{1/2}] \quad (27a)$$

or, equivalently,

$$z = [R - (R^2 - pr^2)^{1/2}]/p, \quad (27b)$$

where $r^2 = x^2 + y^2$.

Since the cornea being modeled has axial symmetry, only one hemimeridian needs to be considered, because the information on all meridia will be identical. The HS array was assumed to have 0.5-mm spacing. Since the distance from the axis to the outer ablation zone is 3.0 mm, there were seven HS sensors in a hemimeridian. This spacing corresponds to 113 sensors within the two-dimensional pupil area. The polynomial used to express corneal shape in Eq. (6) [and in derivatives in Eq. (10)] can be simplified in this axially symmetric case to a one-dimensional power function in even powers of $r^2 = x^2 + y^2$ (odd powers lead to higher-order discontinuities). In the calculations that were done to obtain Fig. 2, powers of up to r^8 were used. In separate calculations it was found that the results were unchanged for exponents from 2 to 10. Also, the results were unchanged by a doubling of the HS sampling density. The robustness of these calculations is not surprising, given the finding of this study that the ablation is insensitive to corneal shape.

The ordinate of Fig. 2 gives the maximum difference between the exact ablation calculation, [Eq. (17)], and the ablation obtained from the simplified calculation [Eq. (22)]. One of the simplifications was that a flat cornea (an infinite apical radius) was assumed. The striking finding, shown in Fig. 2, is that over this very large range of corneal shapes the maximum deviation of ablation depth, 0.25 μm, is very small.

Suppose that one did not know the corneal shape but, instead of using the flat cornea approximation [Eq. (22)], used an average spherical ($p = 1$) shape with a radius of 8 mm, together with the exact calculation. This case is illustrated by the horizontal line drawn in Fig. 2 at the point on the $p = 1$ curve for $R = 8$ mm (shown by the dot). It can be seen that a maximum error of approximately 0.05 μm, relative to that horizontal line, would be possible for the very broad range of corneas that is shown in Fig. 2. This small error is out of a maximum ablation of approximately 60 μm for our example [see Eq. (24)]. This very small error is the basis for our claim that, if the HS aberrations are known, then it is not necessary to know the corneal shape. An error of 0.05 μm is slightly smaller than the typical standard deviation of the HS wave-front error that was found by Liang and Williams[4] in human subjects.

B. Effect of Aberrations on Ablation Depth

A very different picture is obtained if one asks how the ablation amount depends on the aberration structure of the HS data or on the residual aberrations after ablation. In this section it is shown that if the ablation is given an extra amount of oblateness for correcting myopia then one can have the same average refractive power with less ablation. The extra oblateness can come about in two ways: (1) the HS aberrations indicate that the cornea has too much prolateness (it is shaped like a parabola) so that the ablation needs more oblateness than what would have been done without the HS information, or (2) it may be desirable to leave the final cornea with a little extra oblateness as compared with the optimal shape (or an extra prolateness for correcting hyperopia).

Figure 3(a) shows the difference in corneal height from the central vertex to the rim of the 6-mm-diameter ablation zone. For $r = 3$ mm, Eq. (27) gives the difference as

$$\text{height difference:} \quad 3^2/[R + (R^2 - p3^2)^{1/2}]. \quad (28)$$

The solid line is for an ellipsoid whose apical radius is fixed at $R = 7.5$ mm, corresponding to an optical power of 45 D at the vertex (with the keratometric index of 1.3375). The dashed line corresponds to a range of ellipsoids in which R is not fixed, as is discussed in connection with Eq. (31). The abscissa is the p value, henceforth called the oblateness parameter, since increasing p increases the oblateness. An ellipsoid is oblate for p values greater than 1, prolate for p values between 1 and 0, and hyperbolic for p values less than 0. Equation (27a) shows that for $p = 0$ the cornea is a paraboloid. At $p = 0$ (leftmost point of plot) the height is $z = 3^2/2 \times 7.5 = 0.6$ mm (600 μm). For a sphere, $p = 1$ (rightmost point on plot), the height is given by Eq. (27b) as $z = 7.5 - (7.5^2 - 3^2)^{1/2} = 0.626$ mm, as shown on the plot. The point of this fig-

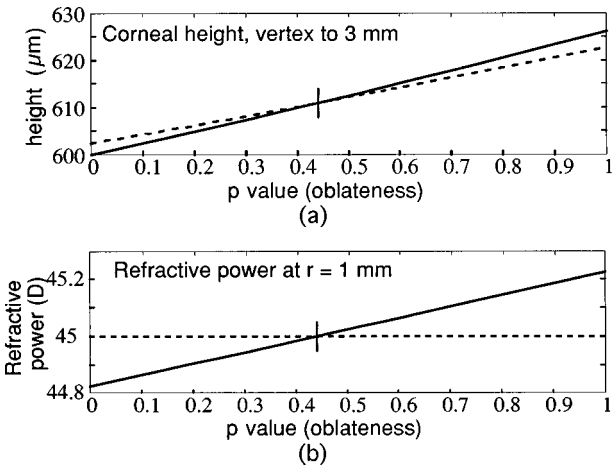

Fig. 3. Effect of oblateness (p value) on the height and refractive power of an ellipsoidal single-surface schematic eye. In both panels the abscissa is the oblateness of the axially symmetric ellipsoid, the solid line is for an ellipsoid whose apical refractive power is 45 D, and the dashed line is for an ellipsoid whose apical power has been adjusted [see Eq. (31)] so that the refractive power $r = 1$ mm is 45 D, where r specifies the distance of the corneal point from the axis. The $r = 1$ mm point is chosen because it is close to the average refractive power across the pupil. The two lines intersect at $p = p_0 = 1 - e^2 = 1 - 1/n^2 = 0.441$, which is the oblateness for an ellipsoid with zero spherical aberration. For this value of p, all corneal points have the same refractive power for incoming axial rays. (a) shows the height (z distance) from the vertex to the ellipsoid at $r = 3$ mm, as given by Eq. (27). The quantity of interest for a myopic correction is the difference in height from $p = p_0$, the optimal postablation value, to a larger oblateness, such as $p = 1$, for a sphere. For a hyperopic correction the relevant height difference would vary from $p = p_0$ to lower values of p. (b) shows the refractive power at $r = 1$ mm. This plot is useful for checking that the change in oblateness does not cause a large change in the refractive power across the optic zone of the cornea.

ure is that, by increasing the oblateness, one increases the corneal height. For the correction of myopia, the central region is ablated more than the peripheral region. Thus, if the final cornea has a larger height (because of its extra oblateness), then less ablation is needed. The point $p = p_0 = 0.441$ has special importance, since it corresponds to the shape of a single-surface eye with optimal refraction, as is discussed in relation to Fig. 3(b) and Eq. (32). As the oblateness changes from the optimal value ($p = 0.441$) to the spherical value ($p = 1$), the solid curve shows the height changes by approximately 15 μm. This is a substantial fraction of the approximately 70 μm of total ablation. It is much greater than the 0.05 μm of error discussed in relation to Fig. 2.

One problem with residual oblateness in a myopic correction is that the oblateness causes the peripheral cornea to have larger power than the apex (think of the spherical aberration of a spherical surface). Thus the ablation did not actually reduce the average refractive power across the cornea as much as the apical power would indicate. Further ablation might be needed for optimal refraction, and the solid line in Fig. 3(a) may be an underestimate of the height change needed for the desired refractive correction. Figure 3(b) provides information regarding the magnitude of the dioptric shift by showing the refractive power 1 mm from the vertex. The 1-mm distance was chosen to indicate an average corneal power, since it is situated between the vertex and the 1.5-mm typical pupil radius.

Figure 3(b) shows the refractive power as a function of the oblateness parameter, p. The refractive power is given by

$$P = n/f, \tag{29}$$

where f is the focal length of the off-axis ray and n is chosen to be 1.3375, giving an apical power of 45 D for $R = 7.5$. The focal length (distance from the corneal vertex to the point at which the ray hits or comes closest to the axis) is[8]

$$f = z + r/\tan(\theta), \tag{30}$$

where θ is the angle that the refracted ray makes with the axis. The two lines in Fig. 3(b) show the refractive power at $r = 1$ mm as a function of the oblateness parameter, p. The solid line in Fig. 3(b) is for the case in which the apical curvature is fixed at 45 D. For this case, as the oblateness increases, the refractive power increases at $r = 1$ mm, as is expected for positive spherical aberration. To keep the power constant at $r = 1$, the apical radius can be increased (thus the apical power decreases) as the oblateness increases, as shown by the dashed line in Fig. 3(b). We found that, if the apical radius is chosen to be

$$R = 7.5 + 0.0666(p - p_0), \tag{31}$$

then the refractive power at $r = 1$ mm is equal to 45 D, to an accuracy of better than 0.0001 D. The optimal oblateness value p_0 (indicated by the vertical line in both panels of Fig. 3) is given by

$$p_0 = 1 - e^2 = 1 - 1/n^2 = 0.441, \tag{32}$$

corresponding to an eccentricity of $e = 1/n$. This value of p generates an ellipsoid that has zero aberrations for a distant, on-axis target. If the oblateness parameter is p_0, then all axial rays (rays parallel to the axis) come to focus at the same point. For an eye that has a constant index of refraction throughout, the above algorithm [Eqs. (1)–(20)] will produce an ellipsoid with $e = 1/n$ ($p = p_0$). This particular ellipsoid is the reference ellipsoid for our discussion about departures from the optimal ablation.

The two lines in Fig. 3(b) intersect at $p = p_0$ because of Eq. (31), which specifies that the apical radius is 7.5 mm at that point for both curves. The power at that point is 45 D, the apical power for the solid line, because with $p = p_0$ all points of the ellipsoid have the same refractive power as the apex.

The dashed line in Fig. 3(a), like the dashed line in Fig. 3(b), is for the ellipsoids whose apical radius has been adjusted by Eq. (31). This adjustment shrinks the height change slightly. In going from the optimal shape to the spherical shape the height difference shifts from 611 to 623 μm. This 12-μm change corresponds to 12 μm of reduced ablation, a substantial amount. The close similarity of the solid and dashed lines in Fig. 3(a) shows that, even for a relatively fixed average power, there is still a substantial reduction in ablation depth as the final surface becomes more oblate.

4. DISCUSSION

A. Comparison of Hartmann–Shack and Alternative Methods for Measuring Aberrations

The variety of methods for measuring the aberrations of the eye can be divided into two categories: object space methods and image space methods. Object space methods measure the beam in object space (the space in front of the eye) on the basis of light starting at a single retinal point. Image space methods examine the aberration pattern on the retina on the basis of light starting from a single object space point.

Two examples of object space methods are the Smirnov method[9–11] and the HS method.[3–5] The Smirnov method adjusts the angle of an incoming beam, through a small patch of cornea, until it is aligned with reference targets (a sensitive hyperacuity task). The HS method, described above, measures the angle of outgoing light coming from a single retinal location and multiple corneal locations.

An important image space method is the Tscherning–Howland[12–14] aberrometer. The Tscherning method[12] places a fine-mesh grid on the cornea, and the subject views defocused light. The grid casts a shadow on the retina. The distorted grid is used to measure the aberrations. Howland and Howland[14] improved the design by using a crossed cylinder of ± 5 D to produce the defocusing.

In principle, it is not possible to exactly predict object space aberrations (light from a single image point) from image space aberrations (light from a single object point), or vice versa. This is because for a given corneal point the two methods use rays with different angles, thereby exploring different portions of the crystalline lens. How-

ever, in practice, the aberrations do not change significantly in the region of interest (the coma and distortion terms are small for the small angles being considered), so the image space and object space methods are equally valid for the purpose of this paper.

B. Ray Optics versus Wave Optics

Two methods are possible for calculating the optimal corneal shape, ray (geometric) optics and wave (physical) optics.[15] The wave optics (Fourier-like) method is described (without equations) by Feynman[16] with his sum-over-paths approach. The ray optics approach, based on Snell's law, has the advantage of being simpler computationally, because for each corneal point only a single ray need be considered, whereas in the wave approach a very large number of rays must be calculated at each corneal point. The disadvantage of the ray optics method is that it is incorrect, being an approximation to the wave optics method. In the present study we make the standard assumption that for smooth surfaces such as the cornea, with pupil diameters greater than 2 mm, the ray methods are sufficiently accurate, and the computationally intensive wave methods can be avoided.

In Section 2, since we calculated the phase of the wave front (step 4) and then propagated that wave front (step 5), it might sound like we are using wave methods. But it is still a ray method, since we are following individual rays while keeping track of phase. For the more exact wave method we would have had to do a Fourier-like integration over the corneal surface and then a second integration over the pupil aperture in the pupil plane.

C. Why Is the Algorithm Relatively Simple?

The formula for calculating ablation is relatively simple for two reasons. First, as already discussed, by specifying the aberrations in terms of the HS information we are able to directly calculate aberrations at the cornea. Second, our main formula, Eq. (17), calculates the quantity D_{c-A}, which is a distance along the ray path from the preablation cornea to the postablation cornea. If we had tried to directly calculate the distance in the z direction, it would have been much more difficult.

D. Correcting the Aberrations with a Contact Lens

The algorithm presented in this paper is for correcting the aberrations by removal of corneal tissue. One could also correct the aberrations by adding tissue, such as by using a contact lens. The one extra complication is that the tear fluid between the contact lens and the cornea must also be taken into account. The algorithm of the present paper is easily adapted to that problem. A closely related algorithm is that of Klein and Barsky,[17] with which one can find the optimal front surface of a contact lens given the shape of the back surface. The eye and tear fluid were assumed to have the same index of refraction. The goal of Klein and Barsky,[17] to find the optimal front surface shape, was the same as the objective of the present study.

E. Minimal Role of Corneal Shape

Figure 2 shows the somewhat surprising result that corneal topography information specifying corneal shape has very little effect on the desired ablation depth for an optimal refraction. The ordinate shows the difference in the maximum ablation depth predicted by the exact algorithm [Eq. (17)] and an algorithm in which the cornea was replaced by a plane [Eq. (22)]. The error was less than 0.25 μm. Figure 2 also shows that the error can be reduced to less than 0.05 μm by use of the exact algorithm together with a typical, rather than exact, corneal shape. The horizontal line in Fig. 2 corresponds to replacement of the true corneal shape with an 8-mm sphere. An error of 0.05 μm is slightly smaller than the typical standard deviation of the HS wave-front error that was found by Liang and Williams[4] in human subjects.

F. Ablation Depth Is Strongly Affected by Aberrations

The pattern of aberrations in either the preablation or the postablation eye has a strong effect on the depth of ablation. Figure 3(a) can be used to estimate how the ablation depth depends on the amount of spherical aberration. If the HS aberration of a myope indicates that the p value (oblateness) is near zero (below the optimal value), then the refractive surgery could safely increase the oblateness with an increase in refractive accuracy and a decrease in ablation depth. If the initial HS aberration is close to the optimal value of $p = 0.441$ (assuming a slightly inaccurate index of refraction of 1.3375), then the oblateness could still be increased to a nearly spherical shape ($p = 1.0$) with minor degradation of refractive sharpness [see Fig. 3(b)] and with an associated reduction in ablation depth. If the initial cornea already had oblate aberrations, then it would be difficult to obtain reduction in ablation depth.

For a hyperope the situation is reversed, since a hyperopic ablation removes more of the peripheral cornea (say, up to 3 mm from the axis) than from the vertex. In that case, in terms of Fig. 3(a), one would want to reduce the height shown on the abscissa by having less oblateness than what the optimal ablation would indicate.

G. Further Research Is Needed

When coma is the dominant[14,18] aberration it is possible to have an oblate shape (increasing curvature) on one hemimeridian and a prolate shape (decreasing curvature) on the opposite hemimeridian. In this case the total ablation depth can be decreased by introduction of a small tilt (prism) to the ablation. One would achieve this by slightly tilting the reference plane that was needed for Eq. (14). Rather than being a constant distance E from the vertex plane ($z = 0$), the reference plane would be a linear function of x and y. A consequence of this tilt is that there would be a small shift in the direction of the line of sight because of the added prism. This would not cause a problem since one adapts to a small amount of prism. Future research is needed to determine whether the reduction in ablation depth is substantial for corneas with typical comalike aberrations.

Further research is also needed on the effect of postablation aberrations on visual acuity for different pupil sizes. This would be similar to the research of Applegate and Gansel,[19] in which visual function (contrast sensitivity function, acuity, glare), corneal topography, and aberrations were measured for different pupil sizes. It is now

possible to extend this research by use of contact lenses with customized front-surface shapes. Lathes are now available for producing contact lenses that are not rotationally symmetric. In the past, accurate psychophysical measurements of the effects of aberrations were not possible for two reasons: (1) The full aberrations of the eye could not be measured accurately, and (2) it was difficult to produce a carefully specified amount of aberrations. Technology has now advanced to the point that both these difficulties can be overcome. It is time to do careful studies on how carefully selected aberrations degrade or do not degrade vision. In addition, it is expected that some amount of aberrations will improve the depth of focus. This effect needs to be carefully explored as well, with the careful control now possible.

Finally, continued research is needed on the healing process and on the biomechanics of thin shells. Although the final shape of the anterior cornea is specified mainly by the amount of ablation, the healing process will modify the final corneal thickness. In myopic PRK surgery, for example, the epithelial regrowth tends to make the central cornea more ablate. Also, the cornea is a thin shell structure under pressure[20]; thus the cornea will stretch slightly in the ablated regions, thereby deforming the shape of the front surface. These factors need to be better understood and taken into account when the optimal ablation is being designed.

REFERENCES AND NOTES

1. G. O. Waring III, "Quality of vision and freedom from optical correction after refractive surgery," J. Refract. Surg. **13**, 213–215 (1997); R. L. Lindstrom, "The Barraquer lecture: surgical management of myopia—a clinician's perspective," J. Refract. Surg. **13**, 287–294 (1997); T. P. Werblin, "20/20—How close must we get?" J. Refract. Surg. **13**, 300–301 (1997).
2. The November 1997 issue of *Optometry and Vision Science* was a special issue on corneal topography containing papers on the state of the art in corneal topography, including several from the corneal topographer manufacturers. R. Mattioli and N. K. Tripoli, "Corneal geometry reconstruction with the Keratron videokeratographer," Optom. Vision Sci. **74**, 881–894 (1997); D. Brenner, "Modeling the cornea with the topographic modeling system videokeratoscope," Optom. Vision Sci. **74**, 895–898 (1997); C. Campbell, "Reconstruction of the corneal shape with the MasterVue Corneal Topography System," Optom. Vision Sci. **74**, 899–905 (1997).
3. J. Liang, B. Grimm, S. Goelz, and J. Bille, "Objective measurement of the wave aberrations of the human eye with the use of a Hartmann–Shack wave-front sensor," J. Opt. Soc. Am. A **11**, 1949–1957 (1994).
4. J. Liang and D. R. Williams, "Aberrations and retinal image quality of the normal human eye," J. Opt. Soc. Am. A **14**, 2873–2883 (1997).
5. J. Liang, D. R. Williams, and D. T. Miller, "Supernormal vision and high-resolution retinal imaging through adaptive optics," J. Opt. Soc. Am. A **14**, 2884–2892 (1997).
6. W. H. Southwell, "Wave-front estimation from wave-front slope measurements," J. Opt. Soc. Am. A **70**, 998–1006 (1980).
7. J. Liang, "A new method to precisely measure the wave aberrations of the human eye with a Hartmann–Shack wavefront sensor," Ph.D. dissertation (Universität Heidelberg, Heidelberg, Germany, 1991).
8. S. A. Klein and R. B. Mandell, "Shape and refractive powers in corneal topography," Invest. Ophthalmol. Visual Sci. **96**, 2096–2109 (1995).
9. M. S. Smirnov, "Measurement of the wave aberration of the human eye," Biophys. J. **7**, 766–795 (1962).
10. M. C. Campbell, E. M. Harrison, and P. Simonet, "Psychophysical measurement of the blur on the retina due to optical aberrations of the eye," Vision Res. **30**, 1587–1602 (1990).
11. R. H. Webb, C. M. Penney, and K. P. Thompson, "Measurement of ocular local wavefront distortion with a spatially resolved refractometer," Appl. Opt. **31**, 3678–3686 (1992).
12. M. Tscherning, "Die monochromatischen Abberationen des menschlichen Auges," Z. Psychol. Physiol. Sinn. **6**, 456–471 (1894).
13. B. Howland and H. C. Howland, "Subjective measurement of high-order aberrations of the eye," Science **193**, 580–582 (1976).
14. H. C. Howland and B. Howland, "A subjective method for the measurement of monochromatic aberrations of the eye," J. Opt. Soc. Am. **67**, 1508–1518 (1977).
15. A. Walther, *The Ray and Wave Theory of Lenses* (Cambridge U. Press, Cambridge, UK, 1995).
16. R. P. Feynman, *QED. The Strange Theory of Light and Matter* (Princeton U. Press, Princeton, N.J., 1985).
17. S. A. Klein and B. A. Barsky, "Method for generating the anterior surface of an aberration-free contact lens for an arbitrary posterior surface," Optom. Vision Sci. **72**, 816–820 (1995).
18. G. Walsh, W. N. Charman, and H. C. Howland, "Objective technique for the determination of monochromatic aberrations of the human eye," J. Opt. Soc. Am. A **1**, 987–992 (1984).
19. R. A. Applegate and K. A. Gansel, "The importance of pupil size in optical quality measurements following radial keratotomy," Refract. Corneal Surg. **6**, 47–54 (1990).
20. H. C. Howland, R. H. Rand, and S. R. Lubkin, "A thin shell model of the cornea and its application to corneal surgery," Refract. Corneal Surg. **8**, 183–186 (1992).